

Prospects for the Determination of H_0 through Observation of Multiply-Imaged Supernovae in Rich Galaxy Cluster Fields

Adam S. Bolton and Scott Burles

*Center for Space Research, Massachusetts Institute of Technology
77 Massachusetts Avenue, Cambridge, MA 02139*

bolton@mit.edu, burles@mit.edu

ABSTRACT

We assess the possibility of carrying out a search for supernovae multiply imaged by rich clusters of galaxies through the phenomenon of gravitational lensing. Time delays between different images of the same event could provide a lensing determination of H_0 complementary to galaxy-QSO lensing studies. We show that relatively low-redshift ($z \sim 0.1$), significantly elliptical clusters can exhibit observationally tractable time delays on the order of a few years despite large lensing mass scales. We find that such a search would be a significant undertaking for current observatories, but that it would be particularly appropriate for a facility such as the proposed Large-aperture Synoptic Survey Telescope.

Subject headings: distance scale—gravitational lensing—galaxies: clusters: general—supernovae: general

1. Introduction

Many authors have considered the scientific potential of gravitationally lensed supernovae (SNe) (Kolatt & Bartelmann 1998; Sullivan et al. 2000; Saini, Raychaudhury, & Shchekinov 2000; Holz 2001; Gal-Yam, Maoz, & Sharon 2002; Oguri, Suto, & Turner 2002, for example). Fourteen years ago, Kovner & Paczyński (1988) contemplated the possibility of observing SNe in galaxies lensed into giant arc images by intervening galaxy clusters. They pointed out that the arrival-time differences between multiple images could be only days to weeks due to the proximity of the SNe to caustic lines in the source plane. Such time delays may be measured with great accuracy, and could yield a robust determination of the Hubble constant if combined with a projected cluster mass model well constrained by other strong lensing features (Kneib et al. 1995; AbdelSalam, Saha, & Williams 1998a,b, for example).

This lensing value for H_0 could avoid the principal difficulties of lensed-QSO-variability H_0 measurements, namely elusive time delays and poorly constrained lens models (Schechter 2000; Kochanek 2002).

The number of known giant-arc clusters is now perhaps large enough to entertain the thought of a targeted search for Kovner and Paczyński’s supernovae. Wu et al. (1998) present a summary of 38 strongly lensing clusters from the literature, containing a total of 48 giant arcs and arclets (see also Williams, Navarro, & Bartelmann (1999)). More recently, Luppino et al. (1999) have reported the discovery of 8 more giant-arc clusters, Gladders, Yee, & Ellingson (2002) 6 more, and Zaritsky & Gonzalez (2002) 3 more. Although we do not pursue this approach here, one could attempt to quantify the total amount of strongly lensed rest-frame ultraviolet luminosity within these known giant arcs, thus allowing an estimate of the associated rest-frame core-collapse SN rate. To do this accurately would require case-by-case lens modeling and arc photometry. A rough estimate is obtained by assuming that each of these 55 clusters strongly lenses a single spiral galaxy with a rest-frame SN rate comparable to that of our own galaxy, which we may take to be approximately one every 50 years (Tammann 1982). A typical arc redshift of $z=1$ would dilate this to one observed SN per source galaxy per century, and thus we might expect one lensed SN every couple of years or so within the current sample of 55 clusters.

With application to the determination of H_0 in mind, this letter explores the prospect of searching for SNe multiply imaged by clusters but not necessarily hosted by giant-arc source galaxies. We note that Lanzetta et al. (2002) argue that above redshifts of ~ 1.5 – 2 , even the Hubble Deep Field observations are insensitive to the surface brightness of most rest-frame ultraviolet emission. We find that such a search would be challenging but not impossible with today’s telescopes and instruments. It would be an ideal project for a large telescope operating in a dedicated survey mode such as the proposed Large-aperture Synoptic Survey Telescope (LSST) (Tyson et al. 2002).

Throughout this letter, we assume a flat, vacuum-dominated cold dark matter (Λ CDM) cosmology with matter and vacuum density parameters $\Omega_M = 0.3$, $\Omega_\Lambda = 0.7$. For the Hubble constant, we take $H_0 = 70 h_{70} \text{ km s}^{-1} \text{ Mpc}^{-1}$ with $h_{70} = 1$.

2. Lensing Theory

Gravitational lensing can be described elegantly through the application of Fermat’s principle (Blandford & Narayan 1986). For a source at (2-vector) angular position $\vec{\beta}$, the

time of arrival relative to the unlensed case for image positions $\vec{\theta}$ is given by

$$t = \frac{(1 + z_L)}{c} \frac{D_L D_S}{D_{LS}} \left[\frac{1}{2} (\vec{\theta} - \vec{\beta})^2 - \psi(\vec{\theta}) \right] , \quad (1)$$

where z_L is the lens redshift, D_L , D_S , and D_{LS} are angular diameter distances to the lens, to the source, and from the lens to the source, and $\psi(\vec{\theta})$ is proportional to the Newtonian potential of the lens projected perpendicular to the line of sight (Narayan & Bartelmann 1996). Images of the source will be seen at positions $\vec{\theta}$ where the arrival time is stationary; that is, at solutions to the “lens equation” obtained by setting the gradient with respect to $\vec{\theta}$ of (1) to zero:

$$\vec{\beta}(\vec{\theta}) = \vec{\theta} - \vec{\nabla}_{\vec{\theta}} \psi(\vec{\theta}) . \quad (2)$$

The scalar magnification μ (the flux ratio of lensed to unlensed images of a source) is given by the ratio of lensed to unlensed differential angular area, thus it is given by the Jacobian determinant of the mapping $\vec{\theta}(\vec{\beta})$ (the local inverse of (2)):

$$\mu = \det \left(\frac{d\theta_i}{d\beta_j} \right) = \left[\det \left(\frac{d\beta_j}{d\theta_i} \right) \right]^{-1} . \quad (3)$$

3. Conditional Cross Sections and Lensing Scales

As a lensing cluster model, we adopt a singular isothermal elliptical mass distribution (SIE). The more familiar singular isothermal sphere (SIS) has a projected mass density proportional to $|\vec{\theta}|^{-1} = (\theta_x^2 + \theta_y^2)^{-1/2}$. If we replace this with a dependence upon $[(1 - \epsilon)\theta_x^2 + (1 + \epsilon)\theta_y^2]^{-1/2}$, we obtain the SIE. Keeton & Kochanek (1998) give a convenient expression for the lensing potential $\psi(\vec{\theta})$ associated with this mass distribution (although our notation differs a bit from theirs). The sole angular scale of the model is set by the “Einstein radius” of the $\epsilon = 0$ (SIS) case:

$$\theta_E = 4\pi \frac{\sigma_v^2}{c^2} \frac{D_{LS}}{D_S} \text{ (radians)} = (28.8 \text{ arcsec}) \left(\frac{\sigma_v}{1000 \text{ km/s}} \right)^2 \frac{D_{LS}}{D_S} , \quad (4)$$

with σ_v being the cluster velocity dispersion (Narayan & Bartelmann 1996).

Our ability to detect multiply-imaged SNe useful for the determination of H_0 will be limited both by attainable depth and maximum tolerable time delay. Accordingly, we define $\sigma(\mu_{\min}, \Delta t_{\max})$ to be the angular cross section in the source plane for lensing into a pair of images with the fainter of the two having (absolute-value) magnification of at least μ_{\min} and the time delay between the two being at most Δt_{\max} . In general, $\sigma(\mu_{\min}, \Delta t_{\max})$ will depend upon source and lens redshifts. However, the scale invariance of the SIE lens model allows

us to generate the function $\sigma(\mu_{\min}, \Delta t_{\max})$ once and rescale it as needed for any source/lens redshift combination.

Let us first obtain $\sigma(\mu_{\min}, \Delta t_{\max})$ for the SIS analytically. If the angular distance β from the source (i.e., SN) position to the lens center is less than θ_E , two images will be observed along a line on the sky through the source position and the lens center: one at a distance $\theta_E + \beta$ from the lens center (in the direction of the source) with magnification $1 + \theta_E/\beta$ and one at a distance $\theta_E - \beta$ (in the direction opposite the source) with magnification $1 - \theta_E/\beta$ (Narayan & Bartelmann 1996). This second, fainter image corresponds to a saddle point of the arrival time function (1); its negative magnification signals a reversal of image parity. It is this magnification that determines the μ_{\min} dependence of $\sigma(\mu_{\min}, \Delta t_{\max})$ as defined. Next, if we substitute the solutions $\theta_E \pm \beta$ into (1) (taking into account vectorial considerations) and form the difference, we find that the time delay between the two images is

$$\Delta t = \frac{2(1 + z_L)}{c} \frac{D_L D_S}{D_{LS}} \theta_E \beta \equiv 2\tau \frac{\beta}{\theta_E} \quad , \quad (5)$$

where we have defined a characteristic lensing timescale by τ as implied. For a cluster velocity dispersion $\sigma_v = 1000$ km/s, τ increases steeply at first with increasing source redshift, then levels off around $\sim 25 h_{70}^{-1}$ years for $z_L = 0.1$ or $\sim 70\text{--}80 h_{70}^{-1}$ years for $z_L = 0.4$.

We see that for the SIS a given β corresponds to a unique Δt as given by (5) and a unique (absolute-value) magnification of $\theta_E/\beta - 1$ for the fainter image, so the form of $\sigma(\mu_{\min}, \Delta t_{\max})$ is particularly simple: we have two singly limited cross sections given by

$$\sigma(\mu_{\min}) = \pi \theta_E^2 (\mu_{\min} + 1)^{-2} \quad (6a)$$

$$\sigma(\Delta t_{\max}) = \frac{1}{4} \pi \theta_E^2 (\Delta t_{\max}/\tau)^2 \quad , \quad (6b)$$

and

$$\sigma(\mu_{\min}, \Delta t_{\max}) = \min [\sigma(\mu_{\min}), \sigma(\Delta t_{\max})] \quad . \quad (7)$$

That is, for a given $(\mu_{\min}, \Delta t_{\max})$, we are either magnification-limited or delay-limited.

Now let us pass from SIS to SIE. The introduction of ellipticity leads to richer lensing phenomena. Most significantly, we acquire a finite cross section for quadruple imaging. Four images of a given source will form if the source position lies within the diamond-shaped (“astroid”) tangential caustic surrounding the lens center (Narayan & Bartelmann 1996). Labeling the images in order of increasing arrival time, 1 and 2 are minima of the arrival time function and 3 and 4 are saddle points. 2 and 3 are in general of much greater absolute magnification than 1 and 4. We now have the possibility of three independent image pairings.

Although the projected SIE lensing potential is analytic as mentioned above, the associated lens equation (2) cannot be solved analytically for all the image positions of an arbitrarily positioned source. Thus to calculate the cross sections of interest in the source plane, we implement a grid-based numerical lens-equation solver with 2D Newton-method solution refinement as described by Schneider, Ehlers, & Falco (1992). With circular symmetry now broken, we would not necessarily expect the doubly limited cross sections for image pairings to be of the form (7), but our numerical calculations show that such a form in fact yields a very good approximation. Figures 1 and 2 show $\sigma(\mu_{\min})$ and $\sigma(\Delta t_{\max})$ for the three independent quad image pairings of least time delay for an SIE lens model with an ellipticity $\epsilon = 0.4$. $\sigma(\mu_{\min}, \Delta t_{\max})$ can then be constructed for each image pairing as per (7). For a given ellipticity, $\sigma(\mu_{\min}, \Delta t_{\max})$ of any quad image pairing is limited by the full angular area of the region in the source plane enclosed by the tangential caustic. This area increases with ellipticity and is approximately $0.1 \theta_E^2$ for $\epsilon = 0.4$ as seen in Figures 1 and 2.

We see from Figures 1 and 2 that the addition of ellipticity significantly increases the cross section for multiple-image lensing with relatively short time delays as compared to the circularly symmetric SIS-lens case, at the cost of reduced magnification. Of the three independent image pairings in the quad case, the 2nd/3rd image pairing is most significant for affording both large magnification and short time delay; these are the two images that will merge and annihilate if the source crosses outside the tangential caustic. If we restrict our attention to lenses with $z_L < \sim 0.1$, the lensing timescale τ as defined in (5) will be $< \sim 25 h_{70}^{-1}$ years for a cluster velocity dispersion $\sigma_v = 1000$ km/s, and all 2nd/3rd image pairings will have time delays of less than $\sim 3 h_{70}^{-1}$ years: an observationally tractable range. Thus the limitation of a maximum tolerable time delay is perhaps not as great an obstacle as initial dimensional analysis suggests.

With all other parameters fixed, both τ and θ_E^2 scale as the fourth power of the cluster velocity dispersion σ_v . Thus if the axes of Figure 2 were labeled in units of years and square arcseconds (instead of in units of τ and θ_E^2), an increase in σ_v would rescale both axes by the same factor. This fact together with the differing concavities of the curves shown in Figure 2 indicates that in delay-limited cases, increasing σ_v will increase an SIE-quad cross section, but decrease an SIS-double cross section.

It may seem unreasonable to consider an ellipticity so great as 0.4. However, the effects of cluster substructure, unmodeled here, are likely to be similar to the effects of increasing cluster ellipticity: higher image multiplicity, shorter time delays between multiple images, and reduced magnification. In fact, ellipticity may be thought of as the leading order of substructure beyond circular symmetry. An obvious refinement would be to carry out the cross section calculation using a more detailed and realistic cluster mass map, but we defer

this possibility to future studies.

4. Accuracy of H_0 Determination

To estimate the usefulness of a hypothetical measured time delay in determining H_0 , we employ a convenient result published by Witt, Mao, & Keeton (2000). In the context of the SIE lens model, the time delay between images A and B is given by

$$\Delta t_{AB} = \frac{1}{2c} \frac{D_L D_S}{D_{LS}} (1 + z_L) \left(|\vec{\theta}_B|^2 - |\vec{\theta}_A|^2 \right) , \quad (8)$$

with the image positions measured relative to the lens center. cH_0^{-1} factors out of the D 's on the right-hand side. The dependence on the cosmological parameters (Ω_M, Ω_Λ) is generally weak but worth noting. For example, taking a lens redshift of 0.1 (0.3) and a source redshift of 1, $D_L D_S / D_{LS}$ changes only by about 1% (3%) as Ω_Λ goes from 0 to 0.7 in flat universes. Assuming the image positions, source and lens redshifts, and time delay can be measured with high accuracy, the greatest source of error in an H_0 determination is due to the uncertainty $\delta \vec{\theta}_0$ in the position of the center of the lens. From (8), this is

$$\frac{\delta H_0}{H_0} = 2 \frac{(\vec{\theta}_B - \vec{\theta}_A) \cdot \delta \vec{\theta}_0}{|\vec{\theta}_B|^2 - |\vec{\theta}_A|^2} \equiv \vec{V} \cdot \delta \vec{\theta}_0 / \theta_E . \quad (9)$$

For positions of 2nd/3rd image pairings obtained numerically, the dimensionless vector \vec{V} ranges in magnitude from 2 for source positions near the lens center to almost zero for source positions just inside the tangential caustic. \vec{V} is approximately of unit magnitude for source positions of area-weighted median fainter-image magnification. The fractional error in an H_0 determination is then roughly equal to the uncertainty (parallel to the image separation vector) of the lens center position in units of the Einstein angular scale θ_E defined in (4). However, the magnification of both images increases as the source approaches the tangential caustic, so a magnification bias favors the detection of events with smaller fractional uncertainties in the derived H_0 .

The preceding analysis assumes that the lensing cluster is in fact an SIE. But in a real cluster field with additional lensing constraints, one would certainly employ a more detailed cluster model. The uncertainty in an H_0 value derived from a lensed SN time delay would then depend upon the details of the uncertainty in the model cluster potential.

5. Predicted Detection Rates

To quantify detection rates we focus on core-collapse (type II) SNe. Assuming a Salpeter IMF with lower and upper mass cutoffs of $0.1 M_\odot$ and $125 M_\odot$ respectively, and that all stars with mass above $8 M_\odot$ result in core-collapse SNe, Madau (1998) derives a conversion factor of 0.0074 between solar masses of star formation and eventual number of type II SNe. The comoving star formation rate density at a given redshift can in turn be related to an observable quantity such as comoving rest-frame ultraviolet luminosity density, which is seen to rise sharply out to the redshifts of $z \sim 1$ that we would hope to probe in our search (Madau, Pozzetti, & Dickinson 1998).

Here we consider two versions of the cosmic star formation rate density as a function of redshift. First, following Sullivan et al. (2000, “SFH-I”), we use the form of Madau & Pozzetti (2000) corrected to a lower mass cutoff of $0.1 M_\odot$ and adjusted from an Einstein-DeSitter (EdS) universe to our assumed Λ CDM cosmology in the manner described by Hogg (2001). This form incorporates an upward correction to account for extinction (Madau 2000; Madau & Pozzetti 2000). We also consider the star formation history reported by Lanzetta et al. (2002) based on their determination of the star formation rate intensity distribution function from redshifts $z = 0$ –10, again converted from EdS to Λ CDM. These authors do not attempt an extinction correction, and we work directly with their “unobscured” star formation rate density.

In principle, we can combine the quadruple-imaging cross sections $\sigma(\mu_{\min}, \Delta t_{\max})$ found for the SIE in Section 3 with these assumed SN rate densities in an integral over source redshifts to obtain an estimate of the detection rates that we might expect:

$$\left(\begin{array}{c} \text{SN image pairings} \\ \text{per cluster} \\ \text{per obs. year} \end{array} \right) = \int_{z_L}^{\infty} \frac{1}{1+z} \dot{\rho}_{\text{SN}}(z) \sigma(\mu_{\min}, \Delta t_{\max}) \frac{dV_C}{d\Omega dz}(z) dz \quad . \quad (10)$$

$dV_C/d\Omega dz$ is the comoving volume per unit solid angle per unit redshift, the angular cross section depends upon source redshift and includes contributions from each of the three independent image pairings, $\dot{\rho}_{\text{SN}}(z)$ is the rate density of core-collapse SNe per unit comoving volume per unit proper time, and the factor of $(1+z)^{-1}$ converts from proper time at the source to observer time. In an actual calculation this integral must be cut off at some upper limit beyond which the supernova rate density becomes utterly unknown.

To obtain a numerical estimate, we assume a $\sigma_v = 1000$ km/s lensing cluster at redshift $z_L = 0.1$ with an ellipticity $\epsilon = 0.4$ (as mentioned above, with the exaggerated ellipticity we hope to approximate the effects of cluster substructure). We take the maximum tolerable observer-frame time delay between multiple images to be $3 h_{70}^{-1}$ years, and investigate a

range of differences between limiting detectable apparent magnitude m_{lim} and SN II absolute magnitude M_{SN} . Figure 3 shows the result of such a detection-rate integration out to a redshift of $z = 8$. If the integration is carried out only to $z = 4$, the high $m_{\text{lim}} - M_{\text{SN}}$ end of the detection rate plot is reduced by $\sim 30\%$ (lower curve) to $\sim 60\%$ (upper curve) for the Lanzetta et al. (2002) star formation rate density, but only by $\sim 10\%$ for the Madau & Pozzetti (2000) rate density, as the former authors report significantly enhanced star formation at high z .

6. Conclusions and Further Considerations

The estimated detection rates shown in Figure 3 allow us to assess the feasibility of a cluster monitor program targeted to detect multiply-imaged SNe. Repeated imaging would be required every month or so, as type II-L (II-P) SNe spend ~ 30 (~ 50) days within one magnitude of maximum light (Doggett & Branch 1985). This time will be stretched by $(1 + z_{\text{SN}})$, but a precise temporal measurement of peak light would be crucial to a time-delay measurement. Taking $m_{\text{lim}} = 25$ and $M_{\text{SN}} = -18$, we would expect at best on the order of a couple of detectable image pairings per cluster per century. A cluster monitor program operating for two to three years would need to image ~ 100 cluster fields to the required depth in order to have a good chance of detecting a few events. Such a program would be feasible with today’s 6–8m-class telescopes with wide-field cameras given several dark nights per month. The project is ideally suited to a telescope such as the proposed LSST, which will operate in a dedicated survey mode, repeatedly imaging large areas of the sky to significant depth.

Although we have considered type II SNe as our sources, a rough idea of the detection rates for type Ia SNe image pairings can be obtained from Figure 3 by assuming that type Ia’s are ~ 10 times less frequent and ~ 1 magnitude brighter than type II’s. Under these assumptions, the prospects are more discouraging than for type II’s. Sullivan et al. (2000) also predict significantly lower detection rates for type Ia’s than for type II’s.

In general, for a given source redshift and lensing cluster velocity dispersion, a lower cluster redshift gives a larger isothermal Einstein radius and a smaller characteristic lensing timescale. Both of these factors argue for targeting lower-redshift clusters in our search. Low-redshift clusters also have more of the (apparently brighter) low-redshift universe behind the them. On the other hand, a larger fraction of the strong-lensing region of the image plane will be masked by cluster galaxies in a lower-redshift cluster, and a cluster core with sub-isothermal projected density may assume a significant angular extent. Presumably there exists some optimal target cluster redshift that balances these considerations, much as there

seems to be an optimal cluster redshift of $z_L \simeq 0.3$ (probably biased by volume effects) for giant-arc lensing (Williams et al. 1999).

Known giant-arc clusters would be obvious targets for a monitor program: they are definitely super-critical, and their projected mass distributions can be significantly constrained through established inversion procedures. For other target clusters without known arcs, a monitor program would yield repeated images of the same field that could be stacked to form a single, very deep image (with the obvious loss of any variability information). Such an image could then be searched for strongly-lensed background features to constrain the cluster mass distribution.

The authors wish to thank Paul Schechter for valuable discussion of these topics.

REFERENCES

- AbdelSalam, H. M., Saha, P., & Williams, L. L. R. 1998, MNRAS, 294, 734
- AbdelSalam, H. M., Saha, P., & Williams, L. L. R. 1998, AJ, 116, 1541
- Blandford, R., & Narayan, R. 1986, ApJ, 310, 568
- Dogget, J. B., & Branch, D. 1985, AJ, 90, 2303
- Gal-Yam, A., Maoz, D., & Sharon, K. 2002, MNRAS, 332, 37
- Gladders, M. D., Yee, H. K. C., & Ellingson, E. 2002, AJ, 123, 1
- Hogg, D. W. 2001, PASP, submitted; also preprint (astro-ph/0105280)
- Holz, D. E. 2001, ApJ, 556, L71
- Keeton, C. R., & Kochanek, C. S. 1998, ApJ, 495, 157
- Kochanek, C. N. 2002, ApJ, submitted; also preprint (astro-ph/0204043)
- Kolatt, T. S., & Bartelmann, M. 1998, MNRAS, 296, 763
- Kovner, I., & Paczyński, B. 1988, ApJ, 335, L9
- Kneib, J.-P., Mellier, Y., Pelló, R., Miralda-Escudé, J., Le Borgne, J.-F., Böhringer, H., & Picat, J.-P. 1995, A&A, 307, 27

- Lanzetta, K. M., Yahata, N., Pascarelle, S., Chen, H.-W., & Fernández-Soto, A. 2002, *ApJ*, 570, 492
- Luppino, G. A., Gioia, I. M., Hammer, F., Le Fèvre, O., & Annis, J. A. 1999, *A&AS*, 136, 117
- Madau, P. 1998, in *ASP Conf. Ser. 146, The Young Universe: Galaxy Formation and Evolution at Intermediate and High Redshift*, ed. S. D’Odorico, A. Fontana, and E. Giallongo (San Francisco: ASP), 289; also preprint (astro-ph/9801005)
- Madau, P., Pozzetti, L., & Dickinson, M. 1998, *ApJ*, 498, 106
- Madau, P. 2000, *PhST*, 85, 156; also preprint (astro-ph/9902228)
- Madau, P., & Pozzetti, L. 2000, *MNRAS*, 312, L9
- Narayan, R., & Bartelmann, M. 1996, preprint (astro-ph/9606001)
- Oguri, M., Suto, Y., & Turner, E. L. 2002, *ApJ*, in press; also preprint (astro-ph/0210107)
- Saini, T. D., Raychaudhury, S., & Shchekinov, Y. A. 2000, *A&A*, 363, 349
- Schechter, P. L. 2002, in *IAU 201*, ed. A. N. Lasenby & A. Wilkinson; also preprint (astro-ph/0009048)
- Schneider, P., Ehlers, J., & Falco, E. E. 1992, *Gravitational Lenses* (Berlin: Springer-Verlag)
- Sullivan, M., Ellis, R., Nugent, P., Smail, I., & Madau, P. 2000, *MNRAS*, 319, 549
- Tammann, G.A. 1982, in *Supernovae: a Survey of Current Research*, ed. M. J. Rees & R. J. Stoneham (Dordrecht: D. Reidel), 371
- Tyson, J. A., Wittman, D. M., Hennawi, J. F., & Spergel, D. N. 2002, for *Proc. 5th International UCLA Symposium on Sources and Detection of Dark Matter*, ed. D. Cline; also preprint (astro-ph/0209632)
- Williams, L. L. R., Navarro, J. F., & Bartelmann, M. 1999, *ApJ*, 527, 535
- Witt, H. J., Mao, S., & Keeton, C. R. 2000, *ApJ*, 544, 98
- Wu, X.-P., Chiueh, T., Fang, L.-Z., & Xue, Y.-J. 1998, *MNRAS*, 301, 861
- Zaritsky, D., & Gonzalez, A. H. 2002, *ApJ*, in press; also preprint (astro-ph/0210352)

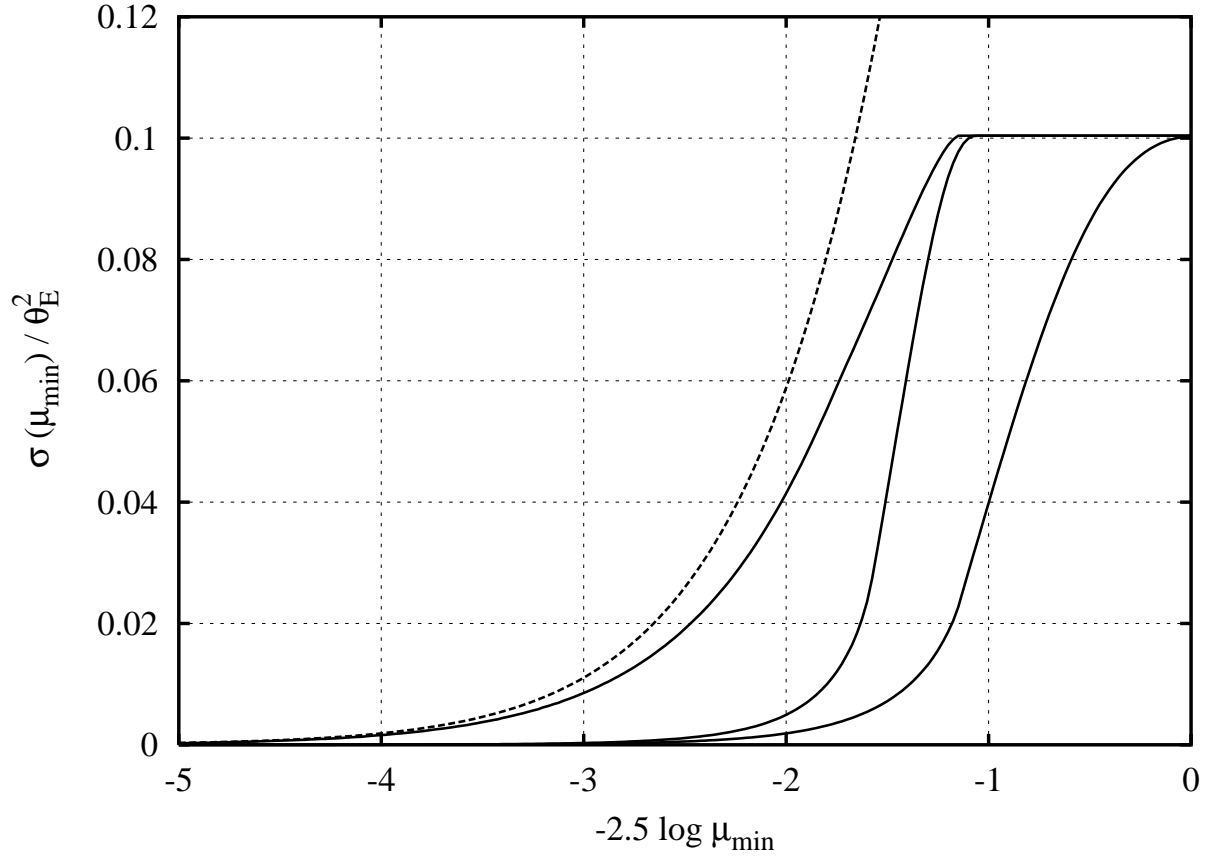


Fig. 1.— Magnification-limited lensing cross sections for an $\epsilon = 0.4$ SIE quad. The upper solid curve corresponds to the 2nd/3rd image pairing, the middle solid curve to the 1st/2nd image pairing, and the lower solid curve to the 3rd/4th. The dashed curve is for the two images of an $\epsilon = 0$ SIS, for comparison.

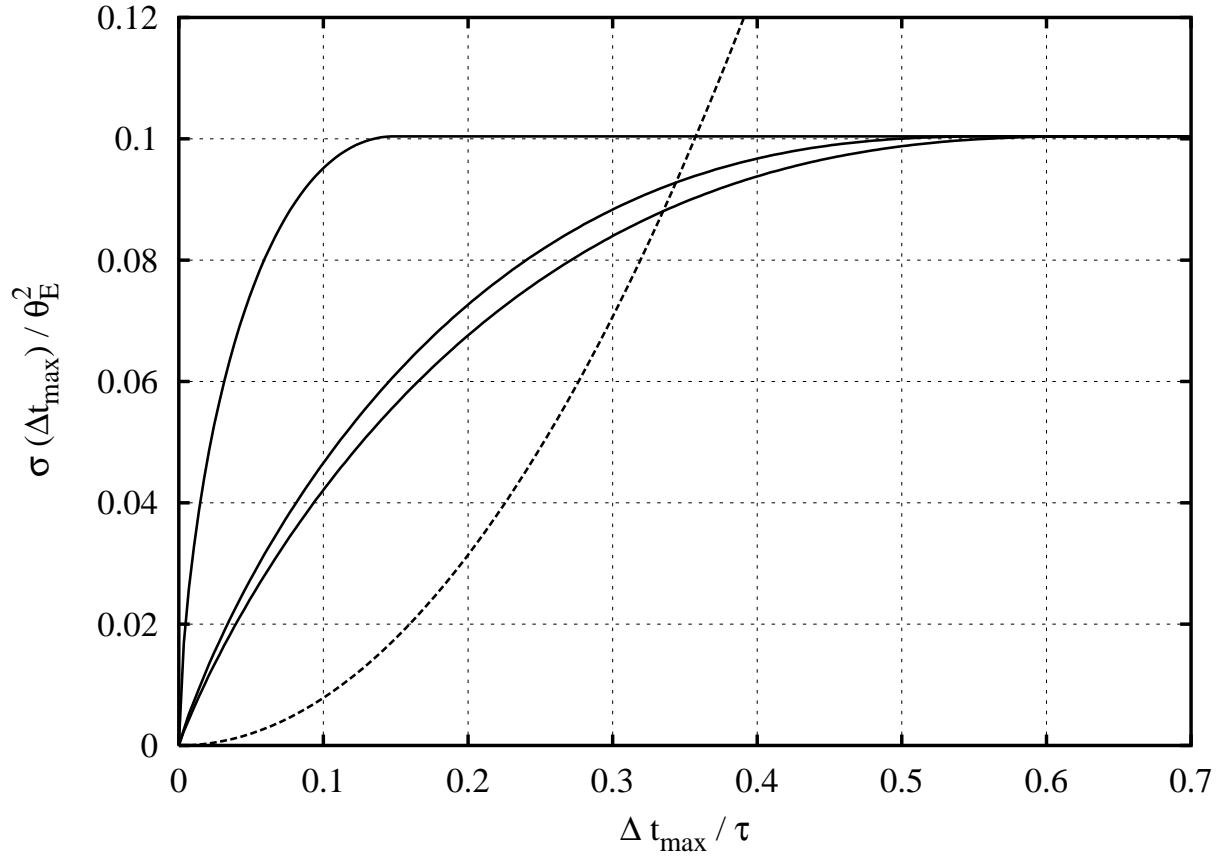


Fig. 2.— Same as Figure 1, but for time-delay limited lensing cross sections.

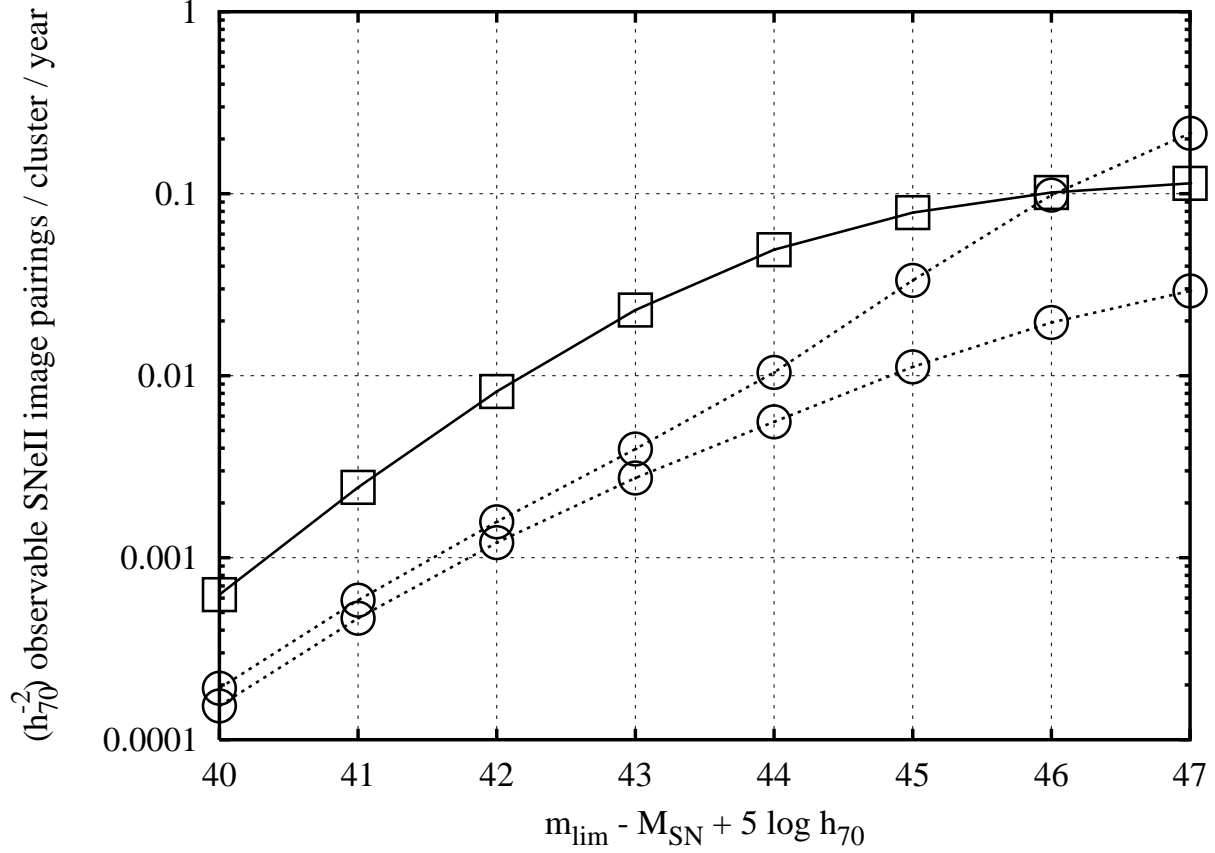


Fig. 3.— Predicted type II SN image pairing detection rates vs. difference between limiting observable magnitude and SN absolute magnitude. ($\sigma_v = 1000$ km/s, $\epsilon = 0.4$ SIE quad; $z_L = 0.1$, maximum observer-frame time delay of $3 h_{70}^{-1}$ years). *Solid line/squares*: star formation rate density of Madau & Pozzetti (2000). *Dashed lines/circles*: star formation rate density of Lanzetta et al. (2002), upper and lower curves.